




Divergent responses of evergreen needle-leaf forests in Europe to the 2020 warm winter

Working Paper

Author(s):

Gharun, Mana; [Shekhar, Ankit](#) ; [Hörtnagl, Lukas](#) ; Krebs, Luana; Arriga, Nicola; Migliavacca, Mirco; Roland, Marilyn; Gielen, Bert; Montagnani, Leonardo; Tomelleri, Enrico; Šigut, Ladislav; Pechl, Matthias; Zhao, Peng; Schmidt, Marius; Grünwald, Thomas; Korkiakoski, Mika; Lohila, Annalea; [Buchmann, Nina](#) 

Publication date:

2024-01-04

Permanent link:

<https://doi.org/10.3929/ethz-b-000663442>

Rights / license:

[Creative Commons Attribution 4.0 International](#)

Originally published in:

EGUsphere, <https://doi.org/10.5194/egusphere-2023-2964>

Funding acknowledgement:

198227 - ICOS-CH Phase 3 (SNF)

173691 - ICOS-CH Phase 2 (SNF)

198094 - Unravel the changing contributions of abiotic vs. biotic drivers of ecosystem gas exchange under weather extremes (SNF)



1 **Divergent responses of evergreen needle-leaf forests in Europe to the 2020 warm winter**

2

3 Mana Gharun¹, Ankit Shekhar², Lukas Hörtnagl², Luana Krebs², Nicola Arriga³, Mirco
4 Migliavacca³, Marilyn Roland⁴, Bert Gielen⁴, Leonardo Montagnani⁵, Enrico Tomelleri⁵,
5 Ladislav Šigut⁶, Matthias Peichl⁷, Peng Zhao⁷, Marius Schmidt⁸, Thomas Grünwald⁹, Mika
6 Korkiakoski¹⁰, Annalea Lohila¹⁰, Nina Buchmann²

7

8 ¹ Institute of Landscape Ecology, University of Münster, Germany

9 ² Department of Environmental Systems Science, Institute of Agricultural Sciences, ETH
10 Zurich, Switzerland

11 ³ European Commission, Joint Research Centre (JRC), Ispra, Italy

12 ⁴ Plants and Ecosystems (PLECO), Department of Biology, University of Antwerp, 2610
13 Wilrijk, Belgium

14 ⁵ Free University of Bolzano, Faculty of Agricultural, Environmental and Food Sciences,
15 39100 Bolzano, Italy

16 ⁶ Global Change Research Institute CAS, Bělidla 986/4a, CZ-60300 Brno, Czech Republic,
17 ORCID: 0000-0003-1951-4100

18 ⁷ Department of Forest Ecology and Management, Swedish University of Agricultural
19 Sciences (SLU), SE-901 83 Umeå, Sweden

20 ⁸ Agrosphere (IBG-3), Institute of Bio- and Geosciences, Jülich Research Centre, 52425
21 Jülich, Germany

22 ⁹ Institute of Hydrology and Meteorology, Technical University of Dresden, Dresden,
23 Germany

24 ¹⁰ Finnish Meteorological Institute, Climate System Research, Helsinki Finland

25

26 Corresponding author: Mana Gharun (mana.gharun@uni-muenster.de)

27

28

29 **Abstract**

30 Relative to drought and heat waves, the effect of winter warming on forest CO₂ fluxes during
31 the dormant season has less been investigated, despite its relevance for net CO₂ uptake in colder
32 regions with higher carbon content in soils. Our objective was to test the effect of the
33 exceptionally warm winter in 2020 on the winter CO₂ budget of cold-adapted evergreen needle-
34 leaf forests across Europe, and identify the contribution of soil and air temperature to changes
35 in winter CO₂ fluxes in response to warming. Our hypothesis was that warming in winter leads
36 to higher emissions across colder sites due to increased ecosystem respiration. To test this
37 hypothesis, we used 98 site-year eddy covariance measurements across 14 evergreen needle-
38 leaf forests (ENFs) distributed from north to south of Europe (from Sweden to Italy). We used
39 a data-driven approach to quantify the effect of air and soil temperature on changes in net
40 ecosystem productivity (NEP) during the warm winter of 2020. Our results showed that the
41 impact of warming was different across sites, as in the lower altitude and lower latitude sites
42 positive soil temperature anomalies were larger, while positive air temperature anomalies were
43 larger in the northern latitude and high-altitude sites. Warming in winter led to a divergent



44 response across the sites. Out of 14 sites only in 3 sites net ecosystem productivity declined in
45 winter significantly in response to warming. In addition, we observed that in the colder sites
46 daytime NEP (that is dominated by photosynthesis) declined with warming of the air in winter,
47 whereas in the warmer sites daytime NEP increased with warming of the soil. While warming
48 increases ecosystem respiration, it might not trigger productivity in winter if the soil within the
49 rooting zone remains frozen. Forests within the same plant functional type category can exhibit
50 differing reactions to winter warming and to predict their responses accurately it is crucial to
51 account for variations in local climate, physiology, and structure simultaneously.

52

53 **Keywords:** eddy covariance, respiration, productivity, long-term, extremes, carbon flux

54

55

56

57 **Introduction**

58 One of the largest sources of uncertainties in understanding how forests can mitigate climate
59 change is the variation of forest CO₂ fluxes in response to extreme climatic conditions. Forests
60 absorb a large part of anthropogenic CO₂ emissions (Friedlingstein et al. 2023), but extreme
61 climatic conditions compromise the capacity of forests for carbon sequestration (Shekhar et al.
62 2023). While a large body of research focuses on extreme events during the growing season,
63 effects of warming winters remain understudied (Kreyling et al. 2019). In northern latitudes
64 and higher altitudes where evergreen conifers dominate, warming events are especially
65 pronounced during the winter months (IPCC 2014). In 2020, Europe experienced its warmest
66 winter on record since 1981 and the largest difference relative to the reference period (1981–
67 2020) was observed in winter over northeastern Europe (Copernicus Climate Change Service
68 2020). However, it is not clear yet how such winter warming affected winter CO₂ fluxes
69 particularly where forests are covered by snow and with high soil C content. Understanding the
70 impact of winter warming on forest net CO₂ uptake requires high temporal resolution
71 observations (sub-seasonal, daily) across many regions, as mechanisms that control forest
72 carbon fluxes are complex and show different responses to changes in climatic conditions,
73 depending on the region and forest type.

74 At the tree level, winter warming could increase CO₂ uptake in temperature-limited forests.
75 While little of this uptake is expected to be allocated to stem growth (Krejza et al. 2022), this
76 increased activity can impact physiological development of plants that are adapted to long cold
77 periods. Plant CO₂ uptake is controlled by a range of physiological responses to light,
78 temperature and CO₂ concentrations. In addition to these external drivers, physiological factors
79 (e.g., photosynthetic parameters such as light-use efficiency, maximum rate of electron



80 transport, maximum carboxylation rate, formation of carbohydrate reserves) and structural
81 characteristics (e.g., leaf area index) which vary across different evergreen needle-leaf forests
82 (ENF), directly affect how productivity and CO₂ uptake might be affected by warming in winter
83 (Martinez Vilalta et al. 2016; Stocker et al. 2018).

84 *Importance of winter period for evergreen needle-leaf forests (ENF)*

85 Forests adapted to cold environments require a persistent number of days with low temperatures
86 for building hardiness. Sudden warming during winter months can promote vegetation activity
87 in response to a condition similar to a “false spring” which can interrupt the cold hardiness
88 process (Laube et al. 2014). Additionally, increased respiration due to warming can deplete
89 stored non-structural carbohydrates (NSC) and tree hydraulic functioning (if combined with
90 drought) and affect tree functioning in spring (Sperling et al. 2015). Winter warming also affects
91 phenological development of trees and increases the chance of photo-oxidative frost damage
92 during earlier stages of the growing season (Gu et al. 2008; Chamberlain et al. 2019). All of
93 this would compromise the capacity of the forest for CO₂ uptake throughout the year (Desai et
94 al. 2016).

95 Environmental cues such as temperature, photoperiod, and light quality control a network of
96 signalling pathways that coordinate cold acclimation and cold hardiness in trees that ensure
97 survival during long periods of low temperature and freezing (Öquist and Hüner 2003;
98 Ensminger et al. 2006). These signalling pathways include the gating of cold responses by the
99 circadian clock, the interaction of light quality and photoperiod, and the involvement of
100 phytohormones in low temperature acclimation (Chang et al. 2021). Soluble carbohydrates,
101 including sucrose (most abundant) accumulate in response to low temperatures, starting from
102 late autumn throughout winter (Strimbeck & Schaberg 2009; Chang et al. 2015). Persistent
103 uninterrupted cold periods thus play an important role in forming the photosynthetic capacity
104 of the trees and their functioning under extreme climatic conditions. Experimental evidence
105 from temperature-sensitive conifers shows that warm spells in winter can induce premature
106 dehardening of buds, and result in stunted shoot development in the following spring (Nørgaard
107 Nielsen & Rasmussen, 2008). In addition to damage from frost, earlier dehardening can
108 potentially affect the capacity of trees to cope with a range of extreme climatic conditions such
109 as cold spells, drought and heat waves.

110 *Effect of warming on forest carbon fluxes*

111 Forest net ecosystem productivity (NEP) depends on the balance between gross ecosystem CO₂
112 uptake (gross primary productivity, GPP) and ecosystem respiration (Reco). Both these flux
113 components are highly sensitive to climate drivers (e.g., air and soil temperature, solar



114 radiation), and thus when canopy structural changes from one year to another are negligible,
115 the interannual variations can be predominantly explained by changes in the climatic conditions
116 (Hui et al. 2003). Net ecosystem productivity can increase or decrease with changes in air
117 temperature. In temperature-limited ecosystems for example, increase in air temperature
118 increases photosynthesis which leads to a larger gross productivity and potentially increased
119 net CO₂ uptake (if respiration does not increase more). However with warming and increased
120 temperatures, respiration (autotrophic and heterotrophic) can also increase, and the balance of
121 this with changes in gross productivity could lead to an increase, no change, or a reduction in
122 net CO₂ uptake (Gharun et al. 2020). In the presence of winter warming, despite more
123 favourable conditions for photosynthesis, factors such as water stress or photoinhibition caused
124 by high photon flux densities in combination with low air temperatures could downregulate
125 photochemical efficiency and negatively affect net photosynthesis which could decline gross
126 primary productivity (Troeng and Linder 1982).

127 The temperature sensitivity of ecosystem respiration regulates how the terrestrial CO₂
128 emissions respond to a warming climate. Within naturally occurring temperature ranges,
129 ecosystem respiration (sum of autotrophic and heterotrophic respirations) typically shows an
130 exponential increase with temperature (Lloyd and Taylor 1994). While previous studies have
131 shown an increase in Q₁₀ (times of increased soil respiration with a 10 °C increase of
132 temperature) with decrease in site mean temperature (e.g., Chen et al. 2020), the temperature
133 sensitivity of ecosystem respiration incorporates both the direct response of ecosystem
134 respiration to temperature and indirect influences from other climatic and physiological
135 variables such as moisture, leaf area index, photosynthate input, litter quality, microbial
136 community (Reichstein et al. 2002; Fierer et al. 2005; Lindroth et al. 2008; Migliavacca et al.
137 2011; Karhu et al. 2014; Collalti et al. 2020). These factors change across species composition
138 and climatic regions and make predicting changes in forest carbon fluxes in response to
139 warming challenging.

140 The winter of 2019-2020 was reported as the hottest on record (1981-2022) across Europe
141 (Copernicus Climate Change Service/ECMWF). When compared to the average conditions, up
142 to 45 less winter ice days were detected in eastern Europe Russe (C3S/KNMI). In Finland, for
143 example, the average air temperature for January and February was over 6 degrees higher than
144 the 1981-2010 mean (Copernicus Climate Change Service/ECMWF). In this study we
145 investigated how the exceptionally warm winter of 2019-2020 affected ENFs in Europe. Our
146 objectives were to:



147 1) evaluate the relative change in air and soil temperature during the winter 2019-2020,
148 compared to a 6-year reference period of 2014-2019, 2) quantify the relative changes in the
149 winter CO₂ fluxes across coniferous sites with available ecosystem-level CO₂ flux
150 measurements, and 3) identify the contribution of climatic drivers (air temperature, soil
151 temperature, solar radiation) to changes in CO₂ fluxes during the warm winter. Our hypothesis
152 was that warming in winter leads to a larger negative effect on net CO₂ balance (i.e., higher
153 emissions) across colder forests. We addressed these objectives and tested our hypothesis by
154 exploring ecosystem-level CO₂ fluxes measured with eddy covariance over 98 site-years in 14
155 evergreen needle-leaf forests distributed from the Boreal to the Mediterranean regions.

156

157 **Material and Methods**

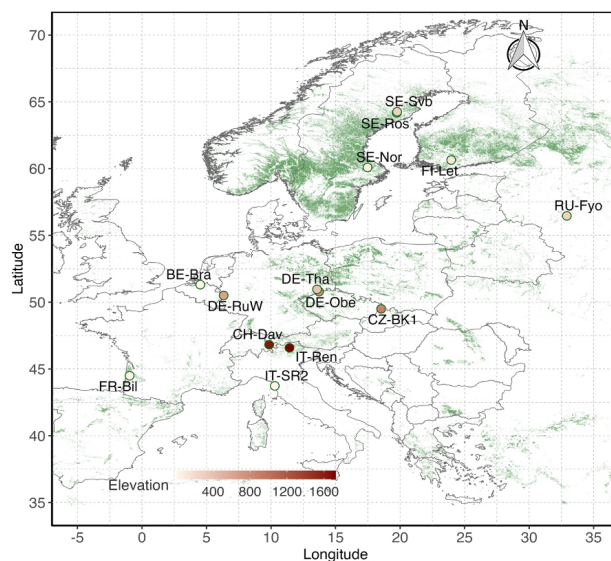
158 *Site description*

159 We selected 14 evergreen needle-leaf forests where continuous CO₂ fluxes and meteorological
160 measurements were available for at least six years until the end of 2020. Selected sites were
161 located from the northern to the southern edge of ENF forest distribution in Europe (Figure 1).

162

163 **Figure 1** Location of the 14 Evergreen Needleleaf Forest (ENF) sites included in this study.
164 Base-map is the MODIS Land Cover Product (MOD12Q1, 500m spatial resolution) showing
165 the distribution of ENFs in Europe in 2020. Elevation of the sites ranges from 4 m a.s.l. (IT-
166 SR2) to 1735 m a.s.l. (IT-Ren).

167



168



169 The most northern site studied is located in Sweden at 64.2 °N (SE-Svb) and the most southern
 170 site in Italy at 43.7 °N (IT-SR2). Mean annual air temperature varies between 1.8 °C (in SE-Ros
 171 and SE-Svb) and 15.4 °C (in IT-SR2) across sites. Mean annual total precipitation varies from 527
 172 mm (in SE-Nor) to 1316 mm (in CZ-BK1). Elevation ranges from 4 m a.s.l. (IT-SR2) to 1730 m
 173 a.s.l. (IT-Ren). Table 1 summarizes the description of sites including their dominant canopy
 174 species.

175

176 **Table 1** Description of the 14 ENF study sites. Mean annual temperature and total precipitation
 177 refer to the 2014-2019 period. Mean number of days with snow cover for each site is based on
 178 the MODIS satellite observations. Sites are listed in a decreasing order in the mean annual
 179 temperature.

180

Site ID	Lat. (°)	Long. (°)	Altitude (m a.s.l.)	Canopy species (dominant first)	Mean annual temperature (°C)	Mean annual precipitation (mm)	Nr days with snow cover
IT-SR2	43.702	10.290	4	<i>Pinus pinea</i>	15.7	950	0
FR-Bil	44.493	-0.956	39	<i>Pinus pinaster</i>	14.1	930	11
BE-Bra	51.307	4.519	16	<i>Pinus sylvestris</i>	11.5	750	20
DE-Tha	50.962	13.565	385	<i>Picea abies</i>	10.2	843	41
DE-RuW	50.504	6.331	610	<i>Picea abies</i>	8.7	1250	50
DE-Obe	50.786	13.721	734	<i>Picea abies</i>	7.4	996	90
SE-Nor	60.086	17.479	45	Mixed (<i>Pinus sylvestris</i> , <i>Picea abies</i>)	7.2	527	89
CZ-Bk1	49.502	18.536	875	<i>Picea abies</i>	7.1	1316	71
RU-Fyo	56.461	32.922	265	Mixed (<i>Picea abies</i> , <i>Betula pubescens</i>)	6.1	711	58
FI-Let	60.641	23.959	111	Mixed (<i>Pinus sylvestris</i> , <i>Picea abies</i> , <i>Betula pubescens</i>)	5.9	627	99
IT-Ren	46.586	11.433	1735	<i>Picea abies</i>	5.5	809	112
CH-Dav	46.815	9.855	1639	<i>Picea abies</i>	4.8	1062	139
SE-Ros	64.172	19.738	160	<i>Pinus sylvestris</i>	4.0	614	102
SE-Svb	64.256	19.774	267	Mixed (<i>Pinus sylvestris</i> , <i>Picea abies</i> , <i>Betula pubescens</i>)	3.2	614	106

181

182 Dataset

183 We used the Warm Winter 2020 eddy covariance dataset processed with FLUXNET pipeline
 184 (compatible with the FLUXNET2015 collection) in this study (Warm Winter 2020 Team, & ICOS
 185 Ecosystem Thematic Centre, 2022); <https://www.icos-cp.eu/data-products/2G60-ZHAK>
 186 (Pastorello et al. 2020). We included the analysis of the spring season at each site to account for



187 the responses immediately after the winter season. Winter months included December, January,
188 and February and spring months included March, April, and May. The 6-year reference period was
189 from 2014 to 2019. This period was selected to have sufficient temporal overlap between the sites.
190 NEE quality-checked with a constant friction velocity (u^*) threshold was used for all sites
191 (NEE_CUT_REF)(Shekhar et al. 2023). For an easier interpretation, we present net ecosystem
192 exchange as net ecosystem productivity (NEP = -NEE) where a negative NEP indicates that forest
193 is a net source, and positive NEP indicates forest is a net sink of CO₂ (Chapin et al. 2006).
194 In terms of climatic variables we selected those that overlapped across all sites during the study
195 period. These included incoming shortwave radiation (R_g), air temperature (T_{air}), soil temperature
196 at 5cm (T_{soil}), precipitation and top soil water content. Given that continuous long-term snow depth
197 measurements were not available at all sites, we used remotely sensed snow depth products to
198 quantify mean snow depth and snow depth anomalies in winter 2020. The snow depth data were
199 derived from the simulation of the Famine Early Warning Systems Network (FEWS NET) Land
200 Data Assimilation System (FLDAS) (McNally et al., 2017). FLDAS data are produced from the
201 Noah version 3.6.1 Land Surface Model (LSM) at a monthly resolution with a global coverage at
202 a spatial resolution of $0.1^\circ \times 0.1^\circ$ (approx. $10 \text{ km} \times 10 \text{ km}$) (Kumar et al., 2013) and has been used
203 in the past to study global spatiotemporal patterns of snow depth and cover (Notarnicola 2022).
204 For snow cover we used MODIS/Terra (MOD10A2) and MODIS/AQUA (MYD10A2) (Hall and
205 Riggs, 2021) Snow Cover 8-Day L3 Global 500m SIN Grid, Version 6 dataset, which provides
206 maximum snow cover extent at 8-day temporal resolution and 500m spatial resolution. For each
207 forest site, we derived average (2014-2019) leaf area index (LAI) from the LAI Collection 300 m
208 Version 1.1 product (LAI300) provided by the Copernicus Global Land Service (Fuster et al.,
209 2020). Average LAI was estimated for each site during the mean net CO₂ uptake period
210 (Supplementary Figure 2). Start of the net carbon uptake period was defined as when daily NEP
211 crosses from negative to positive, and end is the inverse.

212 *Statistical analysis*

213 We compared average daily and daytime (when $R_g > 10 \text{ W/m}^2$ and local time 8-18h) means of
214 each variable (v ; climate drivers, CO₂ fluxes) during the winter and spring of 2020 to the mean
215 from a 6-year reference period (2014-2019) using a t-test ($p < 0.05$). Daily means of each variable
216 was calculated only using the measured and good quality gap-filled half-hourly data (variable
217 quality control = 0 or 1). To understand the major drivers of winter and spring NEP for each forest
218 site, we derived conditional variable importance (CVI _{v}) of each predictor variable (R_g , T_{air} , and
219 T_{soil}) based on a random forest regression model (Breiman, 2001). Soil water content was removed



220 from the drivers analysis because of its negligible effect on the overall model. We tuned the
221 random forest model by iterating ‘ntree’ parameter (number of trees to grow) from 100 to 500 with
222 steps of 50, and ‘mtry’ parameter (number of variables to try at each split) from 1 to 3 with steps
223 of 1, and chose the parameter (ntree = 300 and mtry = 2) with the minimum mean square error.
224 CVI_v accounts for the correlation between the predictor variables, and was calculated using the
225 *party* R-package (Hothorn et al., 2006). Based on a 7-day moving window (centered on the central
226 value of the window) we calculated the mean daily (and daytime) NEP, T_{air} , R_g , and T_{soil} . To
227 compare the CVI_v across sites, for each site we calculated the relative CVI (RCVI) for each
228 variable as per equation 2.

$$229 \quad RCVI_v (\%) = \frac{CVI_v}{\sum CVI_v} \times 100 \quad \text{Equation 2}$$

230 Where $\sum CVI_v$ is the sum of CVI_v of all variables used in the model. We expressed changes in
231 variable during 2020 (v_{2020}) and the reference period ($v_{reference}$) based on its relative anomaly
232 (Δv_r) and absolute anomaly (Δv_a) as per equations 3 & 4.

$$233 \quad \Delta v_r (\%) = \frac{v_{2020} - v_{reference}}{|v_{reference}|} \times 100 \quad \text{Equation 3}$$

$$234 \quad \Delta v_a = v_{2020} - v_{reference} \quad \text{Equation 4}$$

235 To further understand the how (absolute) anomalies of different variables (daytime R_g , T_{air} , T_{soil})
236 explained the variation in daytime ΔNEP , we used the RCVI (as per equation 2) derived from
237 (also) a random forest regression model with hyperparameters $ntree = 100$ and $mtry = 3$ (tuned
238 for lowest mean squared error), for each site (number of data points at least 80 days). The %
239 variance explained of the model was based on the out-of-bag estimates.

240

241 **Results**

242 *Warm winter 2019-2020 conditions across different sites*

243 According to the *in-situ* data, compared to the reference period (2014-2019), winter 2020 was the
244 warmest winter across 10 sites. In seven sites, the winter also had lower precipitation than normal
245 (Figure 2, and Supplementary Figure 1). Positive air temperature anomalies in winter 2020 were
246 larger in the high latitude or high-altitude sites compared to the mid-latitude and low-elevation
247 sites (Figure 3) with largest anomaly of 4.79 °C in RU-Fyo and lowest positive anomaly of 0.87
248 °C observed in IT-SR2 (Figure 3). The average number of snow cover days per year was highly



249 variable across the study sites. (Table 1). The southernmost site studied here (IT-SR2) typically
250 has no snow cover in winter, while the subalpine forest in Switzerland (CH-Dav) has on average
251 139 days with snow (Table 1). In those sites with consistent snow cover in winter (11 out of 14
252 sites) snow depth declined at 9 out of 11 sites during the warm winter of 2020 and reduction was
253 considerable in FI-Let, RU-Fyo, SE-Nor, DE-Obe, DE-Ruw, and DE-Tha (Figure 4). In SE-Svb,
254 FI-Let and DE-Obe soil temperature at 5 cm was continuously above the freezing level in winter
255 2020 (Figure 5), unlike the mean conditions at the sites where soil temperature fluctuates around
256 zero in winter. Changes in winter temperature were more significant in winter than in spring
257 (Figure 3), which is the reason why we focus on the effect of winter warming on CO₂ fluxes only.

258 *Effect of climate drivers on winter CO₂ fluxes*

259 The annual net productivity of ENFs varied from being a maximum sink (\pm sd) of 797 (\pm 320) g C
260 m⁻² yr⁻¹ (CZ-BK1) to a maximum source of -311 (\pm 93) g C m⁻² yr⁻¹ (SE-Nor) during the six-year
261 reference period (2014-2019) (Table 2). Inter-annual variation in NEP was largest in CZ-BK1 (320
262 gC m⁻² yr⁻¹) and lowest in SE-Svb (35 gC m⁻² yr⁻¹) (Table 2). The length of the net CO₂ uptake
263 period was on average 178 days but varied between the sites from 105 days (in RU-Fyo) to 315
264 days (in DE-Ruw) (Table 2, Suppl. Figure 2). Except FR-Bil and DE-RuW all sites were a CO₂
265 source in winter under reference conditions, however in IT-SR2, the forest shifted from a CO₂
266 source into a CO₂ sink in winter 2020 (Supplementary Table 1).

267 During the warm winter 2020, mean daily NEP (i.e., annual winter CO₂ sink or source strength)
268 changed significantly ($p < 0.05$) in 9 out of 14 sites (BE-Bra, CZ-BK1, DE-Obe, FI-Let, IT-Ren,
269 IT-SR2, SE-Svb, SE-Nor, RU-Fyo, grouped as the “affected” sites) compared to the 2014-2019
270 reference period, with changes in both positive and negative directions (Figure 6). For example,
271 in BE-Bra, DE-Obe, IT-Ren, SE-Svb and FI-Let, the forest became a significantly larger source
272 of CO₂ in winter 2020, while in IT-SR2, SE-Nor, CZ-BK1, and RU-Fyo forest shifted towards
273 being a smaller source for CO₂ in winter 2020 (Figure 6, Supplementary Table 1). IT-SR2 showed
274 the largest increased daily NEP in winter (346%) and BE-Bra showed the largest negative anomaly
275 in daily NEP (-97%) (Figure 6). During the warm winter ecosystem respiration (approximated by
276 nighttime NEP) increased significantly across 10 out of 14 sites (Figure 6). Daytime NEP however
277 (dominated by productivity) increased significantly with warming in only 5 sites, and mainly in
278 the warmer sites (Figure 6).

279 The relative importance results of the random forest regression analysis showed that across tested
280 variables, R_g generally had the largest control on NEP. However, with decrease in site baseline
281 (i.e., mean) temperature, the effect of R_g declined (Figure 7). For example, in the three coldest

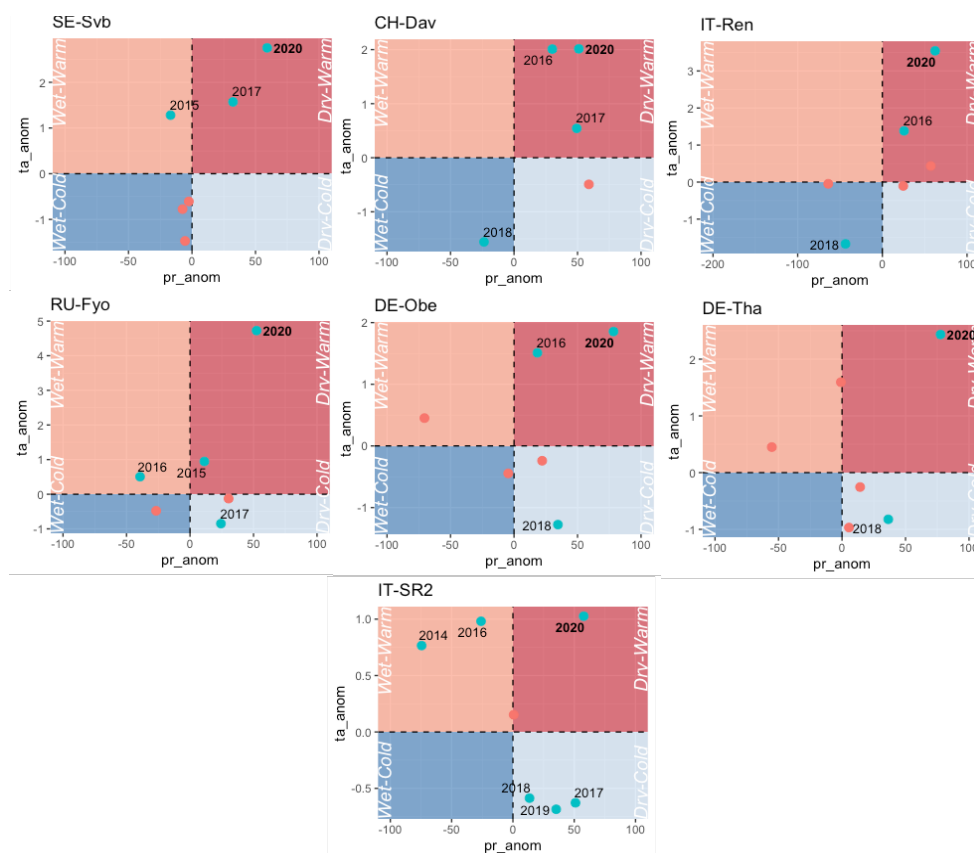


282 sites (SE-Svb, CH-Dav, IT-Ren) R_g had a relative importance of 52%, 23% and 41% for the
 283 variations in NEP respectively, while in the three warmest sites (IT-SR2, FR-Bil and BE-Bra) R_g
 284 had a relative importance of 73%, 81% and 58% for NEP respectively (Figure 7). Radiation
 285 dominated the effect on winter GPP and temperature dominated the effect on winter respiration
 286 fluxes. Particularly in the colder sites the effect of radiation was the least (Figure 7).

287

288

289 **Figure 2** Winter temperature and precipitation anomalies ($x_anom = x - x_mean$) in 2020 (between
 290 December 2019 and February 2020) at those sites where winter 2020 was the warmest and driest
 291 relative to winters during the reference period 2014-2019. Precipitation anomalies are converted
 292 to relative change (relative to mean) but temperature changes are in the original unit (°C).
 293 Anomalies are classified in four main classes of “wet-warm”, “dry-warm”, “wet-cold”, and “dry-
 294 cold”. Winter 2020 is marked in bold. Symbols are marked in blue and label (year) is displayed
 295 only if precipitation change was larger than 10% and at the same time temperature change more
 296 than 0.5 °C. Sites ordered by increasing mean temperature (SE-Svb coldest and IT-SR2 warmest).
 297
 298



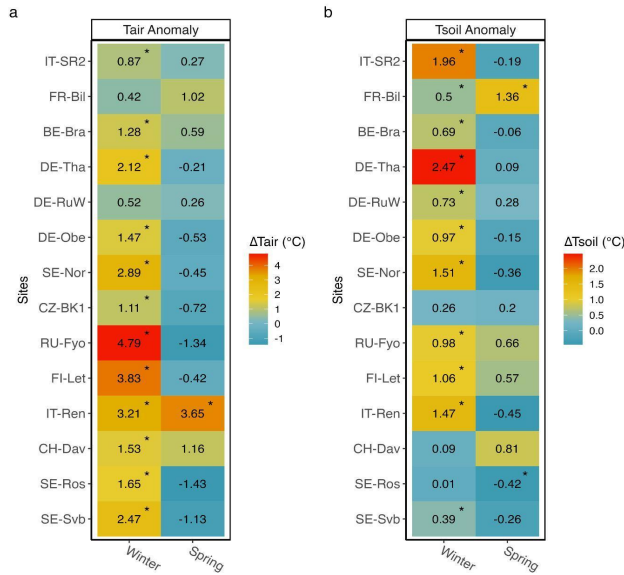
299

300

301



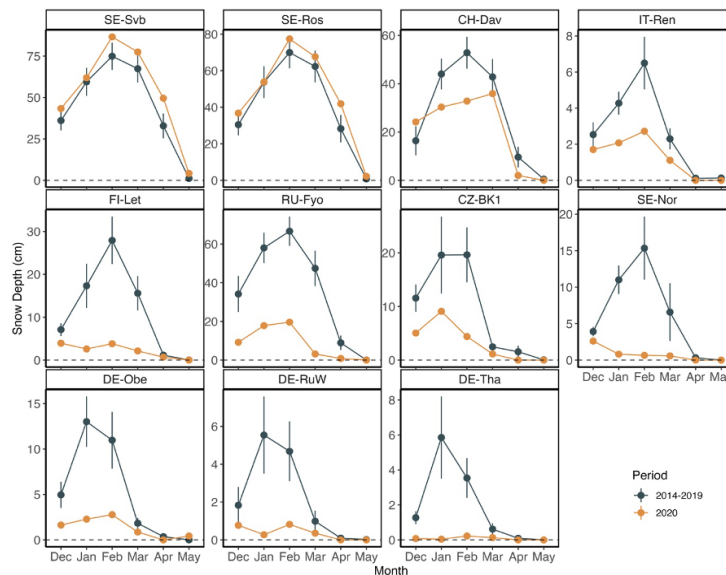
302 **Figure 3** Seasonal changes in air temperature (T_{air}) and soil temperature (T_s) in 2020 compared to
 303 the 6-year reference period (2014-2019). Asterisk marks where means in 2020 were significantly
 304 different from the reference period ($p < 0.05$). Anomalies were calculated from daily values. Sites
 305 are listed in a decreasing order of mean annual air temperature.



306

307

308 **Figure 4** December to May snow depth changes (cm) in winter 2020 compared to the average
 309 winters during the reference period (2014-2019). Note that only 11 out of 14 sites have persistent
 310 snow cover in winter. Sites ordered by increasing mean temperature (SE-Svb coldest and DE-
 311 Tha warmest).
 312



313



314 **Table 2** Mean total annual net ecosystem productivity (NEP) and the standard deviation (inter-
 315 annual variation) during the reference period (2014 and 2019). Start of the net carbon uptake
 316 period (SOS, day of year, DOY) is when daily NEP changes from negative to positive and end
 317 (EOS) is the inverse (see Suppl. Figure 2). Sites are listed in a decreasing order in mean annual
 318 air temperature.
 319

Site ID	NEP (\pm sd) (g C m ⁻² y ⁻¹)	SOS (DOY)	EOS (DOY)	Net carbon uptake period (days)
IT-SR2	197 (\pm 67)	35	200	165
FR-Bil	324 (\pm 103)	20	215	195
BE-Bra	279 (\pm 158)	95	270	175
DE-Tha	484 (\pm 88)	55	305	250
DE-Ruw	597 (\pm 155)	1	365	365
DE-Obe	251 (\pm 147)	75	265	190
SE-Nor	-311 (\pm 93)	90	200	110
CZ-Bk1	797 (\pm 320)	70	310	240
RU-Fyo	25 (\pm 50)	95	200	105
FI-Let	-113 (\pm 123)	100	230	130
IT-Ren	675 (\pm 70)	75	305	230
CH-Dav	231 (\pm 139)	80	280	200
SE-Ros	320 (\pm 136)	95	255	160
SE-Svb	163 (\pm 35)	95	240	145

320

321

322 *Effect of warming on NEP anomalies*

323 Across the low latitude or low altitude (< 1000 m a.s.l.) sites where NEP changed significantly
 324 in winter 2020 (IT-SR2, BE-Bra, DE-Obe), average NEP anomaly was +75%. In the high-
 325 latitude-high elevation sites where NEP was significantly different in winter 2020 (SE-Nor,
 326 CZ-BK1, RU-Fyo, FI-Let, IT-Ren, SE-Svb) the average NEP anomaly was -8.8% (reduced net
 327 uptake) (Figure 6, Supplementary Figure 5). Average variable explained by the random forest
 328 regression for daytime Δ NEP when abiotic drivers were included in winter was 72% in winter
 329 (Figure 8). Across the affected sites, changes in the air temperature dominated the effect on
 330 NEP anomalies (Figure 8). While FI-Let was affected by a partial cut in 2016 (Korkiakoski et
 331 al. 2019; Korkiakoski et al. 2020), winter fluxes remained relatively stable in all pre- and post-
 332 harvest years as the partial cut affected mostly the summer fluxes (data not shown here).
 333 The relationship between air and soil temperature was stronger than radiation and air
 334 temperature across sites and the relationship between air and soil temperature was stronger in
 335 warmer sites (Table 3). In addition to snow cover, leaf area index and the degree of canopy
 336 closure (directly related to LAI) affect the relationship between air and soil temperature through
 337 a stronger shading of the soil in dense forests. CZ-BK1 had the largest LAI (4.52 ± 0.09 se)



338 and SE-Ros the smallest (2.59 ± 0.09). FI-Let had the largest inter-annual variation (± 0.27)
 339 in LAI and IT-Ren and FR-Bil smallest inter-annual variation (± 0.08) (Table 3).

340

341 **Table 3** Pearson correlation coefficient between mean daily incoming shortwave
 342 radiation (R_g), air temperature (T_{air}) and soil temperature at 5m (T_{soil}) at each site during
 343 the reference period (2014-2019). Sites are ordered by a decreasing mean air
 344 temperature. Leaf area index (LAI) values are shown as mean across the study period \pm
 345 standard error of the mean.

346

Site ID	R_g - T_{air}	T_{air} - T_{soil}	LAI \pm se
IT-SR2	0.69	0.97	3.12 (0.11)
FR-Bil	0.65	0.76	3.50 (0.08)
BE-Bra	0.67	0.92	4.42 (0.13)
DE-Tha	0.73	0.96	4.04 (0.19)
DE-RuW	0.59	0.83	2.99 (0.22)
DE-Obe	0.72	0.94	3.69 (0.21)
SE-Nor	0.71	0.90	3.08 (0.09)
CZ-Bkl	0.72	0.92	4.52 (0.09)
RU-Fyo	0.74	0.78	4.06 (0.14)
FI-Let	0.66	0.88	3.29 (0.27)
IT-Ren	0.64	0.84	3.54 (0.08)
CH-Dav	0.63	0.87	3.25 (0.12)
SE-Ros	0.69	0.77	2.59 (0.09)
SE-Svb	0.71	0.84	2.79 (0.12)

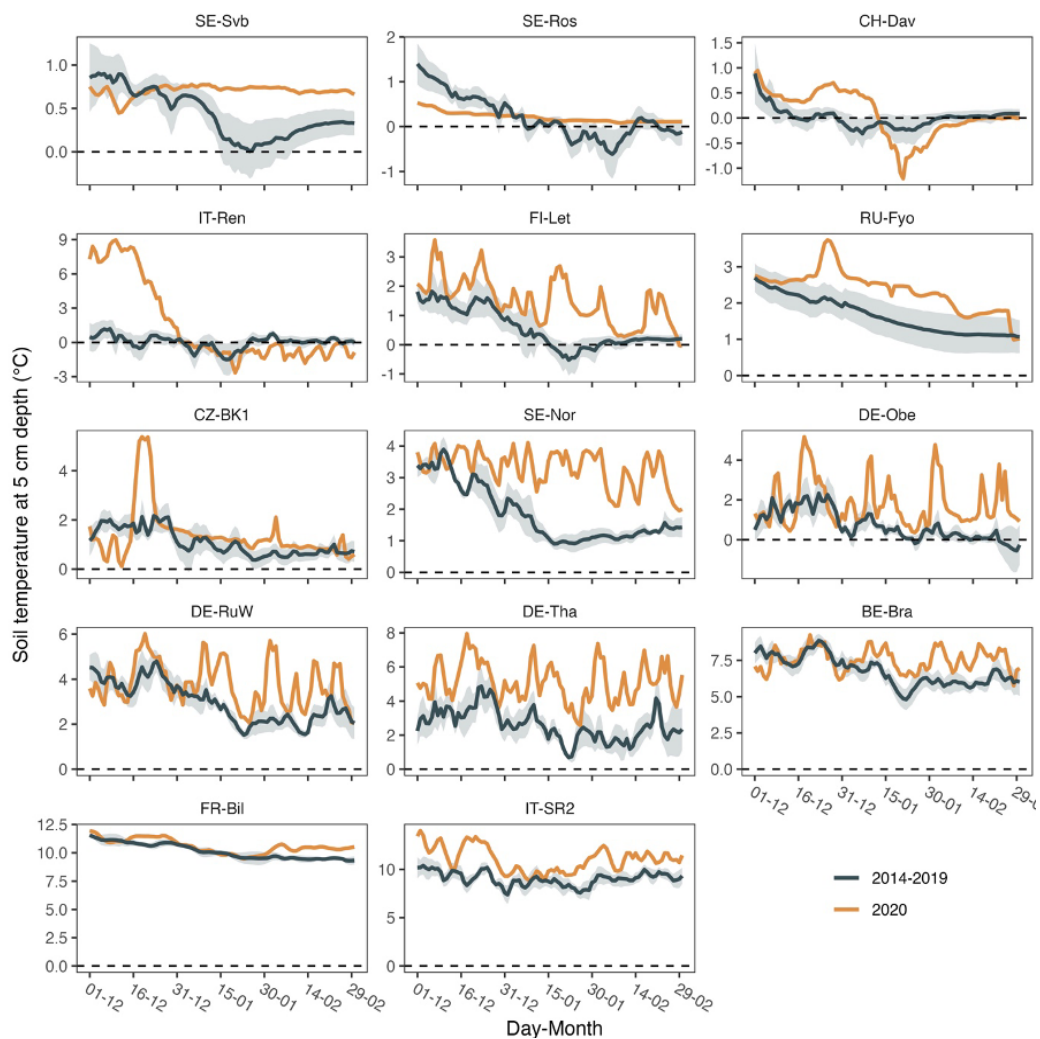
347

348

349

350 **Figure 5** Soil temperature (at 5cm) changes in winter 2020 compared to the reference period
 351 (2014-2019). Shaded bands around the mean show the 95% confidence interval of mean soil
 352 temperature. Sites are ordered (top and right to left) by increasing baseline temperature (SE-
 353 Svb coldest and IT-SR2 warmest).

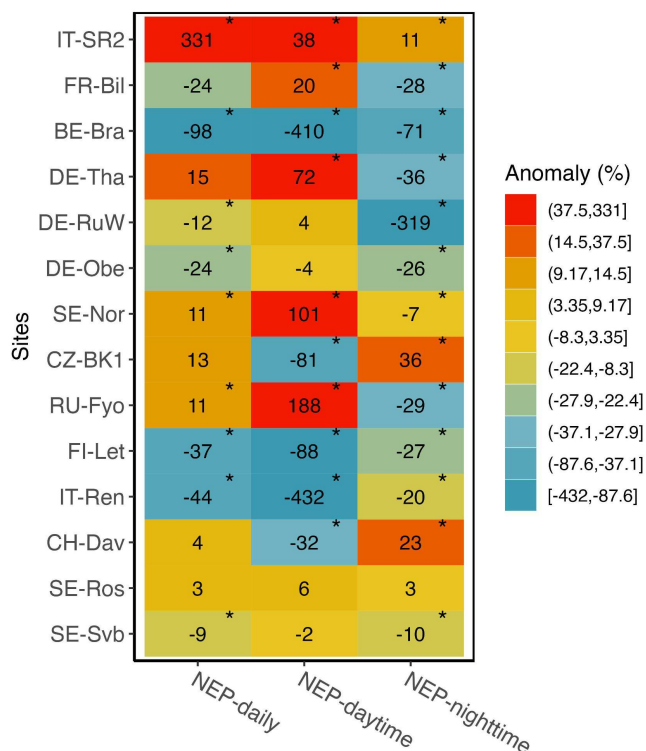
354



355
356
357
358
359
360
361
362
363
364
365
366
367
368
369



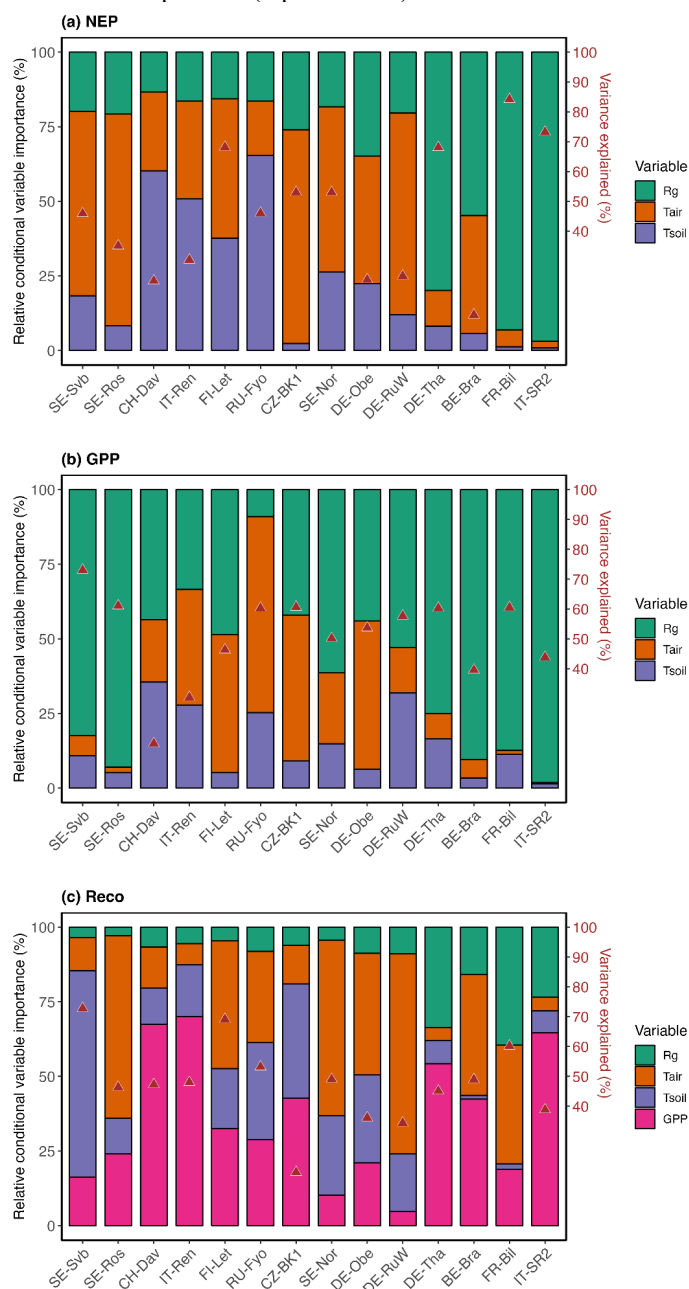
370 **Figure 6** Relative changes (%) in mean daily, nighttime, and daytime NEP in winter 2020
 371 compared to the 6-year reference winters (2014-2019). Asterisks mark where means in 2020
 372 were significantly different from the reference period ($p < 0.05$). Positive NEP change indicates
 373 increased net uptake (due to increased uptake or reduced emission) and negative change
 374 indicates decreased net uptake (due to reduced uptake or increased emission). Sites are listed
 375 in a decreasing mean annual air temperature order.
 376



377
 378
 379
 380
 381
 382
 383
 384
 385
 386
 387
 388
 389
 390
 391
 392
 393



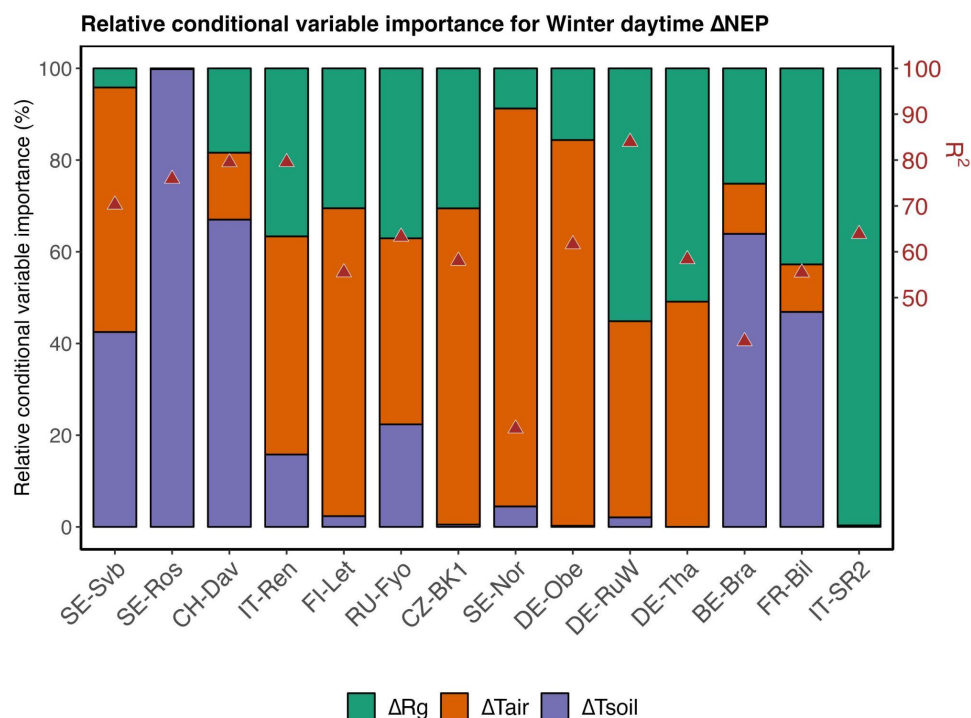
394 **Figure 7** Relative conditional variable importance (RCVI, %) of three climatic variables for
 395 daily winter NEP, GPP and Reco, and the overall variable explained (marked with red
 396 triangles) estimated from the random forest regression analysis. The RFR model was trained
 397 on winter observations during the reference period (2014-2019). The sites are ordered by
 398 decreasing mean annual temperature (top to bottom).



399
400



401 **Figure 8** Comparison of the relative importance of abiotic (T_{air} , R_g , T_s) variables, for NEP
 402 changes (ΔNEP) in winter 2020. R^2 of the RFR model that was used to explain the variation
 403 in daytime ΔNEP (i.e., when PPFD > 0) is shown on the secondary (right) y-axis and marked
 404 with red triangles. Sites are ordered by increasing mean air temperature (from left to right).
 405



406
 407
 408
 409

Discussion

Warming of the air and the soil in winter

410 We tested how climate variables and CO_2 fluxes deviated from a reference period (2014-2019)
 411 during the warm winter of 2020, across 14 evergreen needle-leaf forest sites distributed from
 412 north to south of Europe (from Sweden to Italy). The sites where winter 2020 was particularly
 413 warm and dry were not clustered in a certain climatic region, however we observed a consistent
 414 pattern that warming of the air was more pronounced in the northern latitude and on high
 415 altitudes sites, while in lower latitudes and altitudes warming of the soil was more pronounced
 416 (Figure 3). While in forests top soil temperature is directly affected by changes in the air
 417 temperature, several underlying processes and properties modify the magnitude of decoupling
 418 of air and soil temperature which could reach up to 10 degrees, depending on the season and
 419 properties of the biome type (Lembrechts et al. 2022). These underlying factors and processes
 420



421 include for example 1) a vertically complex and horizontally continuous forest structure that
422 leads to higher decoupling of the soil temperature from air temperature, 2) soil moisture content
423 as moisture increases the soil heat storage, 3) insulation by the litter or snow cover, 4) cloud
424 cover, ground surface albedo, and rate of evapotranspiration which collectively affect the
425 radiation balance and energy exchange between the soil and the air, and 5) microtopography
426 that affects the drainage of air (e.g., cool air drains in low-lying areas) (Guan et al., 2009;
427 Lozano-Parra et al., 2018; De Frenne et al., 2021; Gril et al., 2023). Given that in our study the
428 type of forest was similar across sites (all sites were dominated by evergreen needle-leaf
429 forests) and given that our focus was on the warming during the winter season, we attribute the
430 main source of difference in the soil and air temperature to two main factors. First the snow
431 depth that ranged from no snow to over 100 cm across sites (Table 1, Figure 4), and second,
432 differences in forest structure (e.g. LAI) which varied between 2.59 to 4.52 across the sites
433 (Table 3). We observed that the sites with the smaller snow depth showed a larger warming of
434 the soil during the warm winter of 2020 perhaps because the insulating effect of snow cover
435 was weaker here (Friesen et al. 2021) (Figure 2, Figure 4). At the sites where snow depth
436 declined significantly in winter 2020, soil temperatures increased substantially with large
437 fluctuations over the season, whereas in other sites with greater snow depth such soil
438 temperature fluctuations were absent (Figure 5). The link between warming of the air and
439 warming of the soil was also controlled by the canopy structure as we found a significant
440 positive relationship between the two ($p < 0.05$, $r = 0.69$). Although the direct effect of canopy
441 closure on snow distribution, accumulation and melting at different periods was not tested here,
442 it was evident that sites that had a larger LAI also showed a tighter coupling between air
443 temperature and soil temperature as forest canopy closure reduces snow depth (Table 3)(Woods
444 et al. 2006; Gao et al. 2022).

445 *Winter warming effect on forest CO₂ fluxes*

446 Our general observation was that across sites with a lower mean average temperature (i.e., high
447 altitude or high latitude sites) winter warming was concurrent with increased net CO₂
448 emissions. In the warmer sites however (low altitude or low latitude sites) winter warming also
449 increased the productivity and CO₂ uptake (Supplementary Figure 5). This difference can
450 generally be explained by the balance of changes in the warming of the soil versus warming of
451 the air (Bond-Lamberty and Thomson 2010) which affects both soil respiration and tree CO₂
452 uptake. Where soil becomes proportionally warmer and soil temperature reaches above
453 freezing levels, root activity is enhanced and tree productivity responds directly to the increased



454 air temperatures, and CO₂ uptake increases. Warming of the air - if not translated into a direct
455 warming of the soil- might not enhance productivity if the soil within the rooting zone remains
456 frozen. In IT-Ren for example where daytime NEP declined significantly in the warm winter,
457 air temperature increased to over 3.5 degrees more than normal, however soil temperature
458 remained at freezing levels (Figure 5).

459 CO₂ fluxes are sensitive to changes in both temperature and light (e.g., incoming radiation) and
460 site baseline climate conditions showed to be a good proxy of how changes in light and air
461 temperature lead to changes in NEP (Figure 7). There is however evidence that temperature
462 responses of biochemical processes are a function of plant growth temperature, and not just
463 instantaneous temperature (Fürstenau Togashi et al. 2018). In addition, response of NEP to
464 similar temperature can be different across seasons (i.e., an evident hysteresis), depending on
465 other environmental factors such as solar radiation and soil water content (Niu et al. 2011).
466 While across different sites sensitivity of NEP to temperature increases with a decrease in site
467 mean temperature, as site mean temperature increases (temperature is no longer limiting)
468 radiation becomes a larger constraint on NEP (Running et al. 2004).

469 Chamber-based observations from boreal forests show that snow-depth and soil moisture affect
470 temperature sensitivity of soil CO₂ fluxes as the freeze-thaw cycles abruptly change the
471 moisture content of the soil (Du et al., 2013). In that sense, warmer winters can trigger larger
472 respiration (and availability of nutrients to trees) because of higher Q₁₀ of thawed than frozen
473 soils (Wang et al., 2014), however microbial C limitation can reduce expected increase in
474 respired CO₂, if not countered by greater labile C inputs (Sullivan et al., 2020). In addition,
475 aboveground productivity increases with increase in temperature (Supplementary Figure 3) and
476 enhances the autotrophic respiration. Warming in winter also affects the microbial community
477 that control labile and stable organic carbon decomposition in the soil that would offset
478 respiration response to temperature and lead to a reduction of soil respiration under warming
479 (Tian et al., 2021). The magnitude of increase in belowground autotrophic respiration in
480 response to warming and the supply of labile substrate through rhizodeposition and root
481 exudate also affects net CO₂ fluxes under warming (Nyberg et al., 2020). Decrease in the snow
482 pack and increased soil freezing has short-term immediate impacts on plant CO₂ uptake, but
483 can also leave a long-lasting negative impact on functioning of trees (Repo et al. 2021).
484 Particularly sites with prolonged cold winter seasons could be rather negatively affected by the
485 warming in winter, as we observed through reduced daytime NEP which is an indication of
486 stress from warming during winter. Trees growing in northern latitudes and higher altitudes
487 could be more negatively affected by warming in winter as optimal temperatures in trees are



488 regulated by the short-term changes in temperature, whereas in ecosystems where temperature
489 fluctuations are seasonally larger, optimal temperature for growth has a broader range (Weng
490 et al. 2010; Liu 2020).

491

492 *Winter tree physiology effect on CO₂ fluxes*

493 Responses of coniferous species to soil warming can vary largely depending on the species'
494 adaptive traits, the overall ecosystem context, and interactions with other environmental factors
495 such as precipitation, temperature, and nutrient availability (Dawes et al. 2017; Oddi et al.
496 2022). The sites we studied here, although all were dominated by evergreen needle-leaf species,
497 consisted of different canopy species and some sites were dominated by a mixture of species
498 (Table 1). There can be significant differences in photosynthetic parameters across different
499 species of evergreen conifers that would affect tree and ecosystem response to warming
500 (Fürstenau Togashi et al. 2018). The different responses of productivity to increased warming
501 in ENFs can stem from differences in the quantity (and quality) of stored NSC in the roots, and
502 the rate at which this C storage is mobilized within the tree during the warm winter (Bansal
503 and Germino 2009). Warmer temperatures and dry conditions in winter lead to stomatal closure
504 and depletion of carbohydrate reserves for trees that are adapted to ample precipitation and low
505 VPD conditions in winter, and this effect leads to reduced CO₂ uptake of trees during warmer
506 winters (Earles et al. 2018).

507 Low temperature is essential for signals that trigger the synthesis of soluble carbohydrates
508 involved in osmotic and freezing protection against cold extremes (Chang et al. 2021) that
509 otherwise impair the Calvin cycle by inhibiting the regeneration of ribulose biphosphate
510 (RuBP) and decrease the efficiency of Rubisco carboxylation (Ensminger et al. 2012; Crosatti
511 et al. 2013). Non-structural carbohydrates (sugar and starch) that are accumulated during the
512 growing season are utilized in winter to ensure survival of trees (Zhu et al. 2012; Tixier et al.
513 2020) and failure to develop overwintering defences can cause evergreen conifer needles to
514 remain susceptible for example to photo-oxidative damage during frost events (Chang et al.
515 2016).

516 Our results provide the first analysis of the effect of winter warming on CO₂ fluxes of evergreen
517 needle-leaf forests in Europe and point to the importance of understanding multiple underlying
518 mechanisms that govern CO₂ fluxes. Data on the responses of photosynthetic traits on a
519 timescale that is ecologically relevant (days to years) are scarce, but eddy covariance
520 observations provide an opportunity for constructing long-term time series of canopy level



521 processes to investigate the effect of extreme climatic conditions across all seasons. We
522 encourage studies that combine long-term observations and plant-level experiments to
523 investigate how changes in the functioning in winter might affect trees' response to extremes
524 that occur earlier in the growing season (e.g., spring frost, spring drought) and to understand
525 the consequences of such extremes for ecosystem carbon uptake.

526

527 **Conclusion**

528 Our study investigated the effect of winter warming on CO₂ fluxes of evergreen needle-leaf
529 forests across Europe during the warm 2019-2020 winter. We found significant differences in
530 the impact of warming across sites, with northern and higher-altitude locations experiencing
531 more significant warming of the air, while southern and lower-altitude sites saw greater soil
532 warming. Winter warming influenced forest CO₂ fluxes, with daytime Net Ecosystem
533 Productivity (NEP) decreasing in colder sites due to lower soil temperature, while warmer sites
534 experienced increased CO₂ uptake. However, responses were not similar across all sites, and
535 factors such as forest structure, and local mean climatic conditions played a role in creating
536 microclimates that buffer or enhance the impact of warming on CO₂ fluxes. Understanding
537 these variations combined with tree ecophysiological functioning of cold-adapte ecosystems is
538 crucial for predicting how forests will respond to future winter warming.

539

540 **Acknowledgements**

541 MG acknowledges funding from the Swiss National Science Foundation project ICOS-CH
542 Phase 3 (20FI20_198227). TG acknowledges funding from Free State of Saxony (project
543 'Sicherstellung des Treibhausgasmonitorings an sächsischen ICOS-Standorten') and BMBF
544 (project ICOS-D building phase). BG and RM acknowledge the Research Foundation Flanders
545 (FWO) for the support of ICOS research infrastructure. NB acknowledges funding from the
546 SNF for ICOS-CH Phase 2 (20FI20_173691), and EcoDrive (IZCOŽ0_198094). LŠ was
547 supported by the Ministry of Education, Youth and Sports of CR within the CzeCOS program,
548 grant number LM2023048. We acknowledge the ICOS research infrastructure for data
549 provision.

550

551 *Data availability:* The dataset used in this study is openly available from the ICOS
552 Carbon Portal. <https://doi.org/10.18160/2G60-ZHAK>

553

554 *Author contributions:* MG designed the study; MG and AS performed the data analysis;
555 MG wrote the manuscript, and all authors commented on the analysis and contributed
556 substantially to the writing of the manuscript.

557

558 *Competing interests:* The authors declare that they have no conflict of interests.



559 **References**

- 560 Bansal S, Germino MJ (2009) Temporal variation of nonstructural carbohydrates in montane
561 conifers: similarities and differences among developmental stages, species and
562 environmental conditions. *Tree Physiology* 9(4), 559-568, DOI:
563 10.1093/treephys/tpn045
- 564 Bond-Lamberty, B., Thomson, A. Temperature-associated increases in the global soil
565 respiration record. *Nature* 464, 579–582 (2010). <https://doi.org/10.1038/nature08930>
- 566 Breiman, L. (2001). Random forests. *Machine Learning*, 45(1), 5–32.
567 <https://doi.org/10.1023/A:1010933404324>
- 568 Chamberlain, C. J., Cook, B. I., García de Cortázar-Atauri, I., & Wolkovich, E. M. (2019).
569 Rethinking false spring risk. *Global Change Biology*, 25(7), 2209-2220.
570 doi:<https://doi.org/10.1111/gcb.14642>
- 571 Chang, C. Y., Unda, F., Zubilewich, A., Mansfield, S. D., & Ensminger, I. (2015). Sensitivity
572 of cold acclimation to elevated autumn temperature in field-grown *Pinus strobus*
573 seedlings. *Frontiers in Plant Science*, 6.
- 574 Chang, C. Y., Fréchette, E., Unda, F., Mansfield, S. D., & Ensminger, I. (2016). Elevated
575 temperature and CO₂ stimulate late-season photosynthesis but impair cold hardening in
576 pine. *plant physiology*, 172(2), 802-818.
577 doi:10.1104/pp.16.00753doi:10.3389/fpls.2015.00165
- 578 Chang, C. Y.-Y., Bräutigam, K., Hüner, N. P. A., & Ensminger, I. (2021). Champions of
579 winter survival: cold acclimation and molecular regulation of cold hardiness in
580 evergreen conifers. *New Phytologist*, 229(2), 675-691.
581 doi:<https://doi.org/10.1111/nph.16904>
- 582 Chapin, F.S., Woodwell, G.M., Randerson, J.T. et al. Reconciling Carbon-cycle Concepts,
583 Terminology, and Methods. *Ecosystems* 9, 1041–1050 (2006).
584 <https://doi.org/10.1007/s10021-005-0105-7>
- 585 Chen, J.L., Reynolds, J.F., Harley, P.C. et al. (1993) Coordination theory of leaf nitrogen
586 distribution in a canopy. *Oecologia* 93, 63–69. <https://doi.org/10.1007/BF00321192>
- 587 Chen S, Wang J, Zhang T, Hu Z (2020) Climatic, soil, and vegetation controls of the
588 temperature sensitivity (Q₁₀) of soil respiration across terrestrial biomes. *Global*
589 *Ecology and Conservation* 22, e00955
- 590 Collalti, A. et al. Plant respiration: controlled by photosynthesis or biomass? *Glob. Change*
591 *Biol.* 26, 1739–1753 (2020).
- 592 Crosatti, C., Rizza, F., Badeck, F.-W., Mazzucotelli, E., & Cattivelli, L. (2013). Harden the
593 chloroplast to protect the plant. *Physiologia Plantarum*, 147 1, 55-63.
- 594 Dawes, M.A., Schleppei, P., Hättenschwiler, S., Rixen, C. and Hagedorn, F. (2017), Soil
595 warming opens the nitrogen cycle at the alpine treeline. *Glob Change Biol*, 23: 421-434.
596 <https://doi.org/10.1111/gcb.13365>
- 597 De Frenne, P., Lenoir, J., Luoto, M., Scheffers, B.R., Zellweger, F., Aalto, J., Ashcroft, M.B.,
598 Christiansen, D.M., Decocq, G., De Pauw, K., Govaert, S., Greiser, C., Gril, E., Hampe,
599 A., Jucker, T., Klings, D.H., Koelemeijer, I.A., Lembrechts, J.J., Marrec, R., Meeussen,
600 C., Ogée, J., Tyystjärvi, V., Vangansbeke, P. and Hylander, K. (2021), Forest
601 microclimates and climate change: Importance, drivers and future research agenda. *Glob*



- 602 Change Biol, 27: 2279-2297. <https://doi.org/10.1111/gcb.15569>
- 603 Desai A., G. Wohlfahrt, M.J. Zeeman, G. Katata, W. Eugster, L. Montagnani, D. Gianelle, M.
604 Mauder and H-P Schmid (2016) Montane ecosystem productivity responds more to
605 global circulation patterns than climatic trends. Environmental Research Letters, 11,
606 024013.
- 607 Du E. et al., (2013) Winter soil respiration during soil-freezing process in a boreal forest in
608 Northeast China, Journal of Plant Ecology, Volume 6, Issue 5, Pages 349–357,
609 <https://doi.org/10.1093/jpe/rtt012>
- 610 Earles, J.M., Stevens, J.T., Sperling, O., Orozco, J., North, M.P. and Zwieniecki, M.A.
611 (2018), Extreme mid-winter drought weakens tree hydraulic–carbohydrate systems and
612 slows growth. New Phytol, 219: 89-97. <https://doi.org/10.1111/nph.15136>
- 613 Ensminger, I., Busch, F., & Huner, N. P. A. (2006). Photostasis and cold acclimation: sensing
614 low temperature through photosynthesis. Physiologia Plantarum, 126(1), 28-44.
615 doi:<https://doi.org/10.1111/j.1399-3054.2006.00627.x>
- 616 Ensminger, I., Berninger, F., & Streb, P. (2012). Response of photosynthesis to low
617 temperature. In J. Flexas, F. Loreto, & H. Medrano (Eds.), Terrestrial photosynthesis in
618 a changing environment: a molecular, physiological, and ecological approach (pp. 276–
619 293): UK: Cambridge University Press.
- 620 Fierer, N., Craine, J. M., McLauchlan, K. & Schimel, J. P. Litter quality and the temperature
621 sensitivity of decomposition. Ecology 86, 320–326 (2005).
- 622 Friedlingstein, P., O'Sullivan, M., Jones, M. W., Andrew, R. M., Bakker, D. C. E., Hauck, J.,
623 Landschützer, P., Le Quéré, C., Luijckx, I. T., Peters, G. P., Peters, W., Pongratz, J.,
624 Schwingshackl, C., Sitch, S., Canadell, J. G., Ciais, P., Jackson, R. B., Alin, S. R.,
625 Anthoni, P., Barbero, L., Bates, N. R., Becker, M., Bellouin, N., Decharme, B., Bopp,
626 L., Brasika, I. B. M., Cadule, P., Chamberlain, M. A., Chandra, N., Chau, T.-T.-T.,
627 Chevallier, F., Chini, L. P., Cronin, M., Dou, X., Enyo, K., Evans, W., Falk, S., Feely,
628 R. A., Feng, L., Ford, D. J., Gasser, T., Ghattas, J., Gkritzalis, T., Grassi, G., Gregor, L.,
629 Gruber, N., Gürses, Ö., Harris, I., Hefner, M., Heinke, J., Houghton, R. A., Hurtt, G. C.,
630 Iida, Y., Ilyina, T., Jacobson, A. R., Jain, A., Jarníková, T., Jersild, A., Jiang, F., Jin, Z.,
631 Joos, F., Kato, E., Keeling, R. F., Kennedy, D., Klein Goldewijk, K., Knauer, J.,
632 Korsbakken, J. I., Körtzinger, A., Lan, X., Lefèvre, N., Li, H., Liu, J., Liu, Z., Ma, L.,
633 Marland, G., Mayot, N., McGuire, P. C., McKinley, G. A., Meyer, G., Morgan, E. J.,
634 Munro, D. R., Nakaoka, S.-I., Niwa, Y., O'Brien, K. M., Olsen, A., Omar, A. M., Ono,
635 T., Paulsen, M., Pierrot, D., Pockock, K., Poulter, B., Powis, C. M., Rehder, G.,
636 Resplandy, L., Robertson, E., Rödenbeck, C., Rosan, T. M., Schwinger, J., Séférian, R.,
637 Smallman, T. L., Smith, S. M., Sospedra-Alfonso, R., Sun, Q., Sutton, A. J., Sweeney,
638 C., Takao, S., Tans, P. P., Tian, H., Tilbrook, B., Tsujino, H., Tubiello, F., van der Werf,
639 G. R., van Ooijen, E., Wanninkhof, R., Watanabe, M., Wimart-Rousseau, C., Yang, D.,
640 Yang, X., Yuan, W., Yue, X., Zaehle, S., Zeng, J., and Zheng, B.: Global Carbon Budget
641 2023, Earth Syst. Sci. Data, 15, 5301–5369, <https://doi.org/10.5194/essd-15-5301-2023>,
642 2023.
- 643 Friesen, H.C., Slesak, R.A., Karwan, D.L., Kolka, R.K., (2021) Effects of snow and climate
644 on soil temperature and frost development in forested peatlands in Minnesota, USA.
645 Geoderma 394, 115015.
- 646 Foyer, C.H., Neukermans, J., Queval, G., Noctor, G., Harbinson, J. (2012) Photosynthetic



- 647 control of electron transport and the regulation of gene expression. *J. Exp. Bot.*, 63, pp.
648 1637-1661
- 649 Fürstenau Togashi, H., Prentice, I. C., Atkin, O. K., Macfarlane, C., Prober, S. M.,
650 Bloomfield, K. J., and Evans, B. J. (2018) Thermal acclimation of leaf photosynthetic
651 traits in an evergreen woodland, consistent with the coordination hypothesis,
652 *Biogeosciences*, 15, 3461–3474, <https://doi.org/10.5194/bg-15-3461-2018>.
- 653 Fuster, B., Sánchez-Zapero, J., Camacho, F., García-Santos, V., Verger, A., Lacaze, R.,
654 Weiss, M., Baret, F., & Smets, B. (2020). Quality assessment of PROBA-V LAI,
655 fAPAR and fCOVER collection 300 m products of Copernicus global land service.
656 *Remote Sensing*, 12(6), 1017. <https://doi.org/10.3390/rs1206101>
- 657 Gao, Y., Shen, L., Cai, R., Wang, A., Yuan, F., Wu, J., Guan, D., & Yao, H. (2022). Impact
658 of Forest Canopy Closure on Snow Processes in the Changbai Mountains, Northeast
659 China. *Frontiers in Environmental Science*, 10, Article 929309.
660 <https://doi.org/10.3389/fenvs.2022.929309>
- 661 Gharun, M., Hörtnagl, L., Paul-Limoges, E., Ghiasi, S., Feigenwinter, I., Burri, S.,
662 Marquardt, K., Etzold, S., Zweifel, R., Eugster, W., & Buchmann, N. (2020).
663 Physiological response of Swiss ecosystems to 2018 drought across plant types and
664 elevation. *Philosophical Transactions of the Royal Society B: Biological Sciences*,
665 375(1810), 20190521. <https://doi.org/10.1098/rstb.2019.0521>
- 666 Gril, E., Spicher, F., Greiser, C., Ashcroft, M. B., Pincebourde, S., Durrieu, S., Nicolas, M.,
667 Richard, B., Decocq, G., Marrec, R., & Lenoir, J. (2023). Slope and equilibrium: A
668 parsimonious and flexible approach to model microclimate. *Methods in Ecology and*
669 *Evolution*, 14, 885– 897. <https://doi.org/10.1111/2041-210X.14048>
- 670 Gu L, et al. (2008) The 2007 Eastern US Spring Freeze: Increased Cold Damage in a
671 Warming World?, *BioScience*, Volume 58, Issue 3, March 2008, Pages 253–
672 262, <https://doi.org/10.1641/B580311>
- 673 Guan, X., Huang, J., Guo, N. et al. (2009) Variability of soil moisture and its relationship
674 with surface albedo and soil thermal parameters over the Loess Plateau. *Adv. Atmos.*
675 *Sci.* 26, 692–700. <https://doi.org/10.1007/s00376-009-8198-0>
- 676 Hall, D. K. and G. A. Riggs. MODIS/Terra Snow Cover 8-Day L3 Global 500m SIN Grid,
677 Version 6. 2021, Distributed by NASA National Snow and Ice Data Center Distributed
678 Active Archive Center.
- 679 Hothorn, T., Hornik, K., and Zeileis, A.: Unbiased Recursive Partitioning: A Conditional
680 Inference Framework, *J. Comput. Graph. Stat.*, 15, 651–674,
681 <https://doi.org/10.1198/106186006X133933>, 2006.
- 682 Hui, D., Luo, Y., & Katul, G. (2003). Partitioning interannual variability in net ecosystem
683 exchange between climatic variability and functional change. *Tree Physiology*, 23(7),
684 433-442. doi:10.1093/treephys/23.7.433
- 685 IPCC, 2014: Climate Change 2014: Synthesis Report. Contribution of Working Groups I, II
686 and III to the Fifth Assessment Report of the Intergovernmental Panel on Climate
687 Change [Core Writing Team, R.K. Pachauri and L.A. Meyer (eds.)]. IPCC, Geneva,
688 Switzerland, 151 pp.



- 689 Karhu, K., Auffret, M., Dungait, J. et al. Temperature sensitivity of soil respiration rates
690 enhanced by microbial community response. *Nature* 513, 81–84 (2014).
691 <https://doi.org/10.1038/nature13604>
- 692 Knauer, J., El-Madany, T. S., Zaehle, S., & Migliavacca, M. (2018). Bigleaf-An R package
693 for the calculation of physical and physiological ecosystem properties from eddy
694 covariance data. *PLoS ONE*, 13(8), e0201114. doi:10.1371/journal.pone.0201114
- 695 Korkiakoski M, Tuovinen JP, Penttilä T, Sarkkola S, Ojanen P, Minkkinen K, Rainne J,
696 Laurila T, Lohila A (2019) Greenhouse gas and energy fluxes in a boreal peatland forest
697 after clear-cutting, *Biogeosciences* 16, pp. 3703-3723, 10.5194/bg-16-3703-2019
- 698 Korkiakoski M, Ojanen P, Penttilä I, Minkkinen K, Sarkkola S, Rainne J, Laurila T, Lohila A
699 (2020) Impact of partial harvest on CH₄ and N₂O balances of a drained boreal peatland
700 forest, *Agricultural and Forest Meteorology* 295, 108168,
701 <https://doi.org/10.1016/j.agrformet.2020.108168>
- 702 Krejza, J., Haeni, M., Darenova, E., Foltýnová, L., Fajstavr, M., Světlík, J., ... Zweifel, R.
703 (2022). Disentangling carbon uptake and allocation in the stems of a spruce forest.
704 *Environmental and Experimental Botany*, 196, 104787,
705 <https://doi.org/10.1016/j.envexpbot.2022.104787>
- 706 Kreyling, J., Grant, K., Hammerl, V. et al. (2019) Winter warming is ecologically more
707 relevant than summer warming in a cool-temperate grassland. *Sci Rep* 9, 14632.
708 <https://doi.org/10.1038/s41598-019-51221-w>
- 709 Kumar, S. V. et al. (2013) Multiscale evaluation of the improvements in surface snow
710 simulation through terrain adjustments to radiation. *J. Hydrometeorol.* 14, 220–232.
- 711 Lasslop, G., Reichstein, M., Papale, D., Richardson, A., Arneeth, A., Barr, A., Stoy, P., and
712 Wohlfahrt, G. (2010) Separation of net ecosystem exchange into assimilation and
713 respiration using a light response curve approach: critical issues and global evaluation,
714 *Glob. Change Biol.*, 16, 187–208, <https://doi.org/10.1111/j.13652486.2009.02041.x>
- 715 Laube, J. et al., Chilling outweighs photoperiod in preventing precocious spring development.
716 *Glob. Change Biol.* 20, 170–182 (2014).
- 717 Lembrechts, J. J., van den Hoogen, J., Aalto, J., Ashcroft, M. B., De Frenne, P., Kemppinen,
718 J., Kopecký, M., Luoto, M., Maclean, I. M. D., Crowther, T. W., Bailey, J. J., Haesen, S.,
719 Klings, D. H., Niittynen, P., Scheffers, B. R., Van Meerbeek, K., Aartsma, P.,
720 Abdalaze, O., Abedi, M., ... Lenoir, J. (2022). Global maps of soil temperature. *Global
721 Change Biology*, 28, 3110– 3144. <https://doi.org/10.1111/gcb.16060>
- 722 Lindroth, A. et al. Leaf area index is the principal scaling parameter for both gross
723 photosynthesis and ecosystem respiration of Northern deciduous and coniferous forests.
724 *Tellus B* 60, 129–142 (2008).
- 725 Liu Y. (2020) Optimum temperature for photosynthesis: from leaf- to ecosystem-scale. *Sci
726 Bull* 65(8):601-604. doi: 10.1016/j.scib.2020.01.006.
- 727 Lloyd J, Taylor JA (1994) On the temperature dependence of soil respiration. *Funct. Ecol.*, 8
728 (1994), pp. 315-323



- 729 Lozano-Parra J, Pulido M, Lozano-Fondón C, Schnabel S. (2018) How do Soil Moisture and
730 Vegetation Covers Influence Soil Temperature in Drylands of Mediterranean Regions?
731 Water 10(12):1747. <https://doi.org/10.3390/w10121747>
- 732 Maire V, Martre P, Kattge J, Gastal F, Esser G, Fontaine S, et al. (2012) The Coordination of
733 Leaf Photosynthesis Links C and N Fluxes in C3 Plant Species. PLoS ONE 7(6): e38345.
734 <https://doi.org/10.1371/journal.pone.0038345>
- 735 Martinez Vilalta, J., Sala, A., Asensio, D., Galiano, L., Hoch, Gü., Palacio, S., Piper, F.,
736 Lloret, F.. (2016). Dynamics of non-structural carbohydrates in terrestrial plants: A
737 global synthesis. Ecological Monographs. 86. 10.1002/ecm.1231.
- 738 McNally, A. et al. (2017) A land data assimilation system for sub-Saharan Africa food and
739 water security applications. Sci. Data 4, 170012. <https://doi.org/10.1038/sdata.2017.12>
- 740 Migliavacca, M. et al. Semiempirical modeling of abiotic and biotic factors controlling
741 ecosystem respiration across eddy covariance sites. Glob. Change Biol. 17, 390–409
742 (2011).
- 743 Niu S., Luo Y., Fei S., Montagnani L., Bohrer G., Janssens I.A., Gielen B., Rambal S.,
744 Moors E., Matteucci G., (2011). Seasonal hysteresis of net ecosystem exchange in
745 response to temperature change: patterns and causes. Global Change Biology, 17, 3102-
746 3114, DOI: 10.1111/j.1365-2486.2011.02459.x.
- 747 Nørgaard Nielsen, C. C., & Rasmussen, H. N. (2008). Frost hardening and dehardening in
748 *Abies procera* and other conifers under differing temperature regimes and warm-spell
749 treatments. Forestry: An International Journal of Forest Research, 82(1), 43-59.
750 doi:10.1093/forestry/cpn048
- 751 Notarnicola, C. Overall negative trends for snow cover extent and duration in global
752 mountain regions over 1982–2020. Sci Rep 12, 13731 (2022).
753 <https://doi.org/10.1038/s41598-022-16743-w>.
- 754 Nyberg, M. and Hovenden, M. J. (2020) Warming increases soil respiration in a carbon-rich
755 soil without changing microbial respiratory potential, Biogeosciences, 17, 4405–4420,
756 <https://doi.org/10.5194/bg-17-4405-2020>.
- 757 Öquist, G., & Huner, N. P. A. (2003). Photosynthesis of Overwintering Evergreen Plants.
758 Annual Review of Plant Biology, 54(1), 329-355.
759 doi:10.1146/annurev.arplant.54.072402.115741
- 760 Oddi et al (2022) Contrasting responses of forest growth and carbon sequestration to heat and
761 drought in the Alps, Environ. Res. Lett. 17, 045015, doi:10.1088/1748-9326/ac5b3a
- 762 Pastorello, G., Trotta, C., Canfora, E. et al. The FLUXNET2015 dataset and the ONEFlux
763 processing pipeline for eddy covariance data. Sci Data 7, 225 (2020).
764 <https://doi.org/10.1038/s41597-020-0534-3>
- 765 Reichstein, M. et al. Ecosystem respiration in two Mediterranean evergreen holm oak forests:
766 drought effects and decomposition dynamics. Funct. Ecol. 16, 27–39 (2002).
- 767 Repo, T., Domisch, T., Kilpeläinen, J. et al. Soil frost affects stem diameter growth of
768 Norway spruce with delay. Trees 35, 761–767 (2021). <https://doi.org/10.1007/s00468-020-02074-8>
- 769



- 770 Running SW, Nemani RR, Heinsch FA, Zhao M, Reeves M, Hashimoto H (2004). A
771 Continuous Satellite-Derived Measure of Global Terrestrial Primary Production,
772 BioScience, Volume 54, Issue 6, Pages 547–560, [https://doi.org/10.1641/0006-3568\(2004\)054\[0547:ACSMOG\]2.0.CO;2](https://doi.org/10.1641/0006-3568(2004)054[0547:ACSMOG]2.0.CO;2)
773
- 774 Shekhar, A., Hörtnagl, L., Buchmann, N., & Gharun, M. (2023). Long-term changes in forest
775 response to extreme atmospheric dryness. *Global Change Biology*, 00, 1– 18.
776 <https://doi.org/10.1111/gcb.16846>
- 777 Sperling, O., Earles, J.M., Secchi, F., Godfrey, J., Zwieniecki, M.A. (2015) Frost induces
778 respiration and accelerates carbon depletion in trees. *PLoS ONE* 10(2): e0144124. doi:
779 10.1371/journal.pone.0144124
- 780 Stocker, B.D., Zscheischler, J., Keenan, T.F., Prentice, I.C., Peñuelas, J. and Seneviratne, S.I.
781 (2018), Quantifying soil moisture impacts on light use efficiency across biomes. *New*
782 *Phytol*, 218: 1430-1449. <https://doi.org/10.1111/nph.15123>
- 783 Strimbeck, G. R., & Schaberg, P. G. (2009). Going to extremes: low temperature tolerance
784 and acclimation in temperate and boreal conifers. In M. T. Gusta L.; Wisniewski, K.,
785 (Ed.), *Plant cold hardiness: from the laboratory to the field* (pp. 226-239): Wallingford,
786 Oxfordshire, UK: CABI Publishing.
- 787 Sullivan, P.F., Stokes, M.C., McMillan, C.K. et al. (2020) Labile carbon limits late winter
788 microbial activity near Arctic treeline. *Nat Commun* 11, 4024.
789 <https://doi.org/10.1038/s41467-020-17790-5>
- 790 Tian, J., Zong, N., Hartley, I.P., He, N., Zhang, J., Powlson, D., Zhou, J., Kuzyakov, Y.,
791 Zhang, F., Yu, G. and Dungait, J.A.J. (2021), Microbial metabolic response to winter
792 warming stabilizes soil carbon. *Glob Change Biol*, 27: 2011-2028.
793 <https://doi.org/10.1111/gcb.15538>
- 794 Tixier, A., Guzmán-Delgado, P., Sperling, O. et al. Comparison of phenological traits, growth
795 patterns, and seasonal dynamics of non-structural carbohydrate in Mediterranean tree
796 crop species. *Sci Rep* 10, 347 (2020). <https://doi.org/10.1038/s41598-019-57016-3>
- 797 Troeng E, Linder S (1982) Gas exchange in a 20-year-old stand of Scots pine .1. Net
798 photosynthesis of current and one-year-old shoots within and between seasons, *Physiol.*
799 *Plant*. 54: 15-23.
- 800 Walker et al. (2014) The relationship of leaf photosynthetic traits – V_{cmax} and J_{max} – to leaf
801 nitrogen, leaf phosphorus, and specific leaf area: a meta-analysis and modeling study.
802 *Ecology and Evolution* 2014 4(16): 3218– 3235
- 803 Warm Winter 2020 Team, & ICOS Ecosystem Thematic Centre. (2022). Warm Winter 2020
804 ecosystem eddy covariance flux product for 73 stations in FLUXNET-Archive format—
805 release 2022-1 (Version 1.0). ICOS Carbon Portal. <https://doi.org/10.18160/2G60-ZHAK>
806
- 807 Wang, Y., et al. (2014), Non-growing-season soil respiration is controlled by freezing and
808 thawing processes in the summer monsoon-dominated Tibetan alpine grassland, *Global*
809 *Biogeochem. Cycles*, 28, 1081– 1095, doi:10.1002/2013GB004760.
- 810 Weng, Jen-Hsien & Liao, T.-S. (2010). Photosynthetic responses and acclimation to
811 temperature in seven conifers grown from low to high elevations in subtropical Taiwan.
812 *Taiwan Journal of Forest Science*. 25. 117-127.



- 813 Woods, S. W., Ahl, R., Sappington, J., and McCaughey, W. (2006). Snow Accumulation in
814 Thinned Lodgepole Pine Stands, Montana, USA. *For. Ecol. Manag.* 235 (1-3), 202–211.
815 doi:10.1016/j.foreco.2006.08.013
- 816 Wullschleger, S.D. (1993) Biochemical limitations to carbon assimilation in C3 plants - a
817 retrospective analysis of the A/Ci curves from 109 species. *J. Exp. Bot.*, 44, pp. 907-920
- 818 Zhu WZ, Xiang JS, Wang SG, Li MH (2012) Resprouting ability and mobile carbohydrate
819 reserves in an oak shrubland decline with increasing elevation on the eastern edge of the
820 Qinghai-Tibet Plateau. *For Ecol Manage* 278:118–1